

Experimental constraints on the possible J^{PC} quantum numbers of the $X(3872)$

K. Abe,⁹ K. Abe,⁴⁷ I. Adachi,⁹ H. Aihara,⁴⁹ K. Aoki,²³ K. Arinstein,² Y. Asano,⁵⁴
 T. Aso,⁵³ V. Aulchenko,² T. Aushev,¹³ T. Aziz,⁴⁵ S. Bahinipati,⁵ A. M. Bakich,⁴⁴
 V. Balagura,¹³ Y. Ban,³⁶ S. Banerjee,⁴⁵ E. Barberio,²² M. Barbero,⁸ A. Bay,¹⁹ I. Bedny,²
 U. Bitenc,¹⁴ I. Bizjak,¹⁴ S. Blyth,²⁵ A. Bondar,² A. Bozek,²⁹ M. Bračko,^{9,21,14}
 J. Brodzicka,²⁹ T. E. Browder,⁸ M.-C. Chang,⁴⁸ P. Chang,²⁸ Y. Chao,²⁸ A. Chen,²⁵
 K.-F. Chen,²⁸ W. T. Chen,²⁵ B. G. Cheon,⁴ C.-C. Chiang,²⁸ R. Chistov,¹³ S.-K. Choi,⁷
 Y. Choi,⁴³ Y. K. Choi,⁴³ A. Chuvikov,³⁷ S. Cole,⁴⁴ J. Dalseno,²² M. Danilov,¹³ M. Dash,⁵⁶
 L. Y. Dong,¹¹ R. Dowd,²² J. Dragic,⁹ A. Drutskoy,⁵ S. Eidelman,² Y. Enari,²³ D. Epifanov,²
 F. Fang,⁸ S. Fratina,¹⁴ H. Fujii,⁹ N. Gabyshev,² A. Garmash,³⁷ T. Gershon,⁹ A. Go,²⁵
 G. Gokhroo,⁴⁵ P. Goldenzweig,⁵ B. Golob,^{20,14} A. Gorišek,¹⁴ M. Grosse Perdekamp,³⁸
 H. Guler,⁸ R. Guo,²⁶ J. Haba,⁹ K. Hara,⁹ T. Hara,³⁴ Y. Hasegawa,⁴² N. C. Hastings,⁴⁹
 K. Hasuko,³⁸ K. Hayasaka,²³ H. Hayashii,²⁴ M. Hazumi,⁹ T. Higuchi,⁹ L. Hinz,¹⁹ T. Hojo,³⁴
 T. Hokuue,²³ Y. Hoshi,⁴⁷ K. Hoshina,⁵² S. Hou,²⁵ W.-S. Hou,²⁸ Y. B. Hsiung,²⁸
 Y. Igarashi,⁹ T. Iijima,²³ K. Ikado,²³ A. Imoto,²⁴ K. Inami,²³ A. Ishikawa,⁹ H. Ishino,⁵⁰
 K. Itoh,⁴⁹ R. Itoh,⁹ M. Iwasaki,⁴⁹ Y. Iwasaki,⁹ C. Jacoby,¹⁹ C.-M. Jen,²⁸ R. Kagan,¹³
 H. Kakuno,⁴⁹ J. H. Kang,⁵⁷ J. S. Kang,¹⁶ P. Kapusta,²⁹ S. U. Kataoka,²⁴ N. Katayama,⁹
 H. Kawai,³ N. Kawamura,¹ T. Kawasaki,³¹ S. Kazi,⁵ N. Kent,⁸ H. R. Khan,⁵⁰
 A. Kibayashi,⁵⁰ H. Kichimi,⁹ H. J. Kim,¹⁸ H. O. Kim,⁴³ J. H. Kim,⁴³ S. K. Kim,⁴¹
 S. M. Kim,⁴³ T. H. Kim,⁵⁷ K. Kinoshita,⁵ N. Kishimoto,²³ S. Korpar,^{21,14} Y. Kozakai,²³
 P. Krizan,^{20,14} P. Krokovny,⁹ T. Kubota,²³ R. Kulasiri,⁵ C. C. Kuo,²⁵ H. Kurashiro,⁵⁰
 E. Kurihara,³ A. Kusaka,⁴⁹ A. Kuzmin,² Y.-J. Kwon,⁵⁷ J. S. Lange,⁶ G. Leder,¹²
 S. E. Lee,⁴¹ Y.-J. Lee,²⁸ T. Lesiak,²⁹ J. Li,⁴⁰ A. Limosani,⁹ S.-W. Lin,²⁸ D. Liventsev,¹³
 J. MacNaughton,¹² G. Majumder,⁴⁵ F. Mandl,¹² D. Marlow,³⁷ H. Matsumoto,³¹
 T. Matsumoto,⁵¹ A. Matyja,²⁹ Y. Mikami,⁴⁸ W. Mitaroff,¹² K. Miyabayashi,²⁴ H. Miyake,³⁴
 H. Miyata,³¹ Y. Miyazaki,²³ R. Mizuk,¹³ D. Mohapatra,⁵⁶ G. R. Moloney,²² T. Mori,⁵⁰
 A. Murakami,³⁹ T. Nagamine,⁴⁸ Y. Nagasaka,¹⁰ T. Nakagawa,⁵¹ I. Nakamura,⁹
 E. Nakano,³³ M. Nakao,⁹ H. Nakazawa,⁹ Z. Natkaniec,²⁹ K. Neichi,⁴⁷ S. Nishida,⁹
 O. Nitoh,⁵² S. Noguchi,²⁴ T. Nozaki,⁹ A. Ogawa,³⁸ S. Ogawa,⁴⁶ T. Ohshima,²³ T. Okabe,²³
 S. Okuno,¹⁵ S. L. Olsen,⁸ Y. Onuki,³¹ W. Ostrowicz,²⁹ H. Ozaki,⁹ P. Pakhlov,¹³ H. Palka,²⁹
 C. W. Park,⁴³ H. Park,¹⁸ K. S. Park,⁴³ N. Parslow,⁴⁴ L. S. Peak,⁴⁴ M. Pernicka,¹²
 R. Pestotnik,¹⁴ M. Peters,⁸ L. E. Piilonen,⁵⁶ A. Poluektov,² F. J. Ronga,⁹ N. Root,²
 M. Rozanska,²⁹ H. Sahoo,⁸ M. Saigo,⁴⁸ S. Saitoh,⁹ Y. Sakai,⁹ H. Sakamoto,¹⁷
 H. Sakaue,³³ T. R. Sarangi,⁹ M. Satapathy,⁵⁵ N. Sato,²³ N. Satoyama,⁴² T. Schietinger,¹⁹
 O. Schneider,¹⁹ P. Schönmeier,⁴⁸ J. Schümann,²⁸ C. Schwanda,¹² A. J. Schwartz,⁵
 T. Seki,⁵¹ K. Senyo,²³ R. Seuster,⁸ M. E. Sevier,²² T. Shibata,³¹ H. Shibuya,⁴⁶ J.-G. Shiu,²⁸
 B. Shwartz,² V. Sidorov,² J. B. Singh,³⁵ A. Somov,⁵ N. Soni,³⁵ R. Stamen,⁹ S. Stanič,³²
 M. Starič,¹⁴ A. Sugiyama,³⁹ K. Sumisawa,⁹ T. Sumiyoshi,⁵¹ S. Suzuki,³⁹ S. Y. Suzuki,⁹
 O. Tajima,⁹ N. Takada,⁴² F. Takasaki,⁹ K. Tamai,⁹ N. Tamura,³¹ K. Tanabe,⁴⁹
 M. Tanaka,⁹ G. N. Taylor,²² Y. Teramoto,³³ X. C. Tian,³⁶ S. N. Tovey,²² K. Trabelsi,⁸

Y. F. Tse,²² T. Tsuboyama,⁹ T. Tsukamoto,⁹ K. Uchida,⁸ Y. Uchida,⁹ S. Uehara,⁹
 T. Uglov,¹³ K. Ueno,²⁸ Y. Unno,⁹ S. Uno,⁹ P. Urquijo,²² Y. Ushiroda,⁹ G. Varner,⁸
 K. E. Varvell,⁴⁴ S. Villa,¹⁹ C. C. Wang,²⁸ C. H. Wang,²⁷ M.-Z. Wang,²⁸ M. Watanabe,³¹
 Y. Watanabe,⁵⁰ L. Widhalm,¹² C.-H. Wu,²⁸ Q. L. Xie,¹¹ B. D. Yabsley,⁵⁶ A. Yamaguchi,⁴⁸
 H. Yamamoto,⁴⁸ S. Yamamoto,⁵¹ Y. Yamashita,³⁰ M. Yamauchi,⁹ Heyoung Yang,⁴¹
 J. Ying,³⁶ S. Yoshino,²³ Y. Yuan,¹¹ Y. Yusa,⁴⁸ H. Yuta,¹ S. L. Zang,¹¹ C. C. Zhang,¹¹
 J. Zhang,⁹ L. M. Zhang,⁴⁰ Z. P. Zhang,⁴⁰ V. Zhilich,² T. Ziegler,³⁷ and D. Zürcher¹⁹

(The Belle Collaboration)

¹*Aomori University, Aomori*

²*Budker Institute of Nuclear Physics, Novosibirsk*

³*Chiba University, Chiba*

⁴*Chonnam National University, Kwangju*

⁵*University of Cincinnati, Cincinnati, Ohio 45221*

⁶*University of Frankfurt, Frankfurt*

⁷*Gyeongsang National University, Chinju*

⁸*University of Hawaii, Honolulu, Hawaii 96822*

⁹*High Energy Accelerator Research Organization (KEK), Tsukuba*

¹⁰*Hiroshima Institute of Technology, Hiroshima*

¹¹*Institute of High Energy Physics,*

Chinese Academy of Sciences, Beijing

¹²*Institute of High Energy Physics, Vienna*

¹³*Institute for Theoretical and Experimental Physics, Moscow*

¹⁴*J. Stefan Institute, Ljubljana*

¹⁵*Kanagawa University, Yokohama*

¹⁶*Korea University, Seoul*

¹⁷*Kyoto University, Kyoto*

¹⁸*Kyungpook National University, Taegu*

¹⁹*Swiss Federal Institute of Technology of Lausanne, EPFL, Lausanne*

²⁰*University of Ljubljana, Ljubljana*

²¹*University of Maribor, Maribor*

²²*University of Melbourne, Victoria*

²³*Nagoya University, Nagoya*

²⁴*Nara Women's University, Nara*

²⁵*National Central University, Chung-li*

²⁶*National Kaohsiung Normal University, Kaohsiung*

²⁷*National United University, Miao Li*

²⁸*Department of Physics, National Taiwan University, Taipei*

²⁹*H. Niewodniczanski Institute of Nuclear Physics, Krakow*

³⁰*Nippon Dental University, Niigata*

³¹*Niigata University, Niigata*

³²*Nova Gorica Polytechnic, Nova Gorica*

³³*Osaka City University, Osaka*

³⁴*Osaka University, Osaka*

³⁵*Panjab University, Chandigarh*

³⁶*Peking University, Beijing*

³⁷*Princeton University, Princeton, New Jersey 08544*

³⁸*RIKEN BNL Research Center, Upton, New York 11973*

³⁹*Saga University, Saga*

⁴⁰*University of Science and Technology of China, Hefei*

⁴¹*Seoul National University, Seoul*

⁴²*Shinshu University, Nagano*

⁴³*Sungkyunkwan University, Suwon*

⁴⁴*University of Sydney, Sydney NSW*

⁴⁵*Tata Institute of Fundamental Research, Bombay*

⁴⁶*Toho University, Funabashi*

⁴⁷*Tohoku Gakuin University, Tagajo*

⁴⁸*Tohoku University, Sendai*

⁴⁹*Department of Physics, University of Tokyo, Tokyo*

⁵⁰*Tokyo Institute of Technology, Tokyo*

⁵¹*Tokyo Metropolitan University, Tokyo*

⁵²*Tokyo University of Agriculture and Technology, Tokyo*

⁵³*Toyama National College of Maritime Technology, Toyama*

⁵⁴*University of Tsukuba, Tsukuba*

⁵⁵*Utkal University, Bhubaneswer*

⁵⁶*Virginia Polytechnic Institute and State University, Blacksburg, Virginia 24061*

⁵⁷*Yonsei University, Seoul*

Abstract

We examine possible J^{PC} quantum number assignments for the $X(3872)$. Angular correlations between final state particles in $X(3872) \rightarrow \pi^+\pi^- J/\psi$ decays are used to rule out J^{PC} values of 0^{++} and 0^{-+} . The shape of the $\pi^+\pi^-$ mass distribution near its upper kinematic limit favors S -wave over P -wave as the relative orbital angular momentum between the final-state dipion and J/ψ , which strongly disfavors 1^{-+} and 2^{-+} assignments. The accumulated evidence strongly favors a $J^{PC} = 1^{++}$ assignment for the $X(3872)$, although the 2^{++} possibility is not ruled out by tests reported here. The analysis is based on a sample of $X(3872)$ mesons produced via the exclusive process $B \rightarrow KX(3872)$ in a 256 fb^{-1} data sample collected at the $\Upsilon(4S)$ resonance in the Belle detector at the KEKB collider.

PACS numbers: 14.40.Gx, 12.39.Mk, 13.20.He

The $X(3872)$ was first observed by Belle in exclusive $B^- \rightarrow K^- \pi^+ \pi^- J/\psi$ decays [1, 2]. The subsequent observation of the $X(3872) \rightarrow \gamma J/\psi$ decay mode [3] established the charge parity as $C = +1$. In the same paper, Belle also reported evidence for the decay $X \rightarrow \pi^+ \pi^- \pi^0 J/\psi$, where the $\pi^+ \pi^- \pi^0$ invariant mass distribution has a strong peak between 750 MeV and the kinematic limit of 775 MeV, suggesting that the process is dominated by the sub-threshold decay $X \rightarrow \omega J/\psi$. The partial widths for $3\pi J/\psi$ and $2\pi J/\psi$ decays are of comparable size, which implies a large violation of isospin symmetry.

Here we report on a study of $X(3872) \rightarrow \pi^+ \pi^- J/\psi$ decays produced via the exclusive decay process $B \rightarrow K X(3872)$. We use a data sample that contains 275 million $B\bar{B}$ pairs collected in the Belle detector at the KEKB energy-asymmetric e^+e^- collider. The data were accumulated at a center-of-mass system (cms) energy of $\sqrt{s} = 10.58$ GeV, corresponding to the mass of the $\Upsilon(4S)$ resonance. KEKB is described in detail in ref. [4].

The Belle detector is a large-solid-angle magnetic spectrometer that consists of a three-layer silicon vertex detector, a 50-layer cylindrical drift chamber (CDC), an array of aerogel threshold Cherenkov counters (ACC), a barrel-like arrangement of time-of-flight scintillation counters (TOF), and an electromagnetic calorimeter (ECL) comprised of CsI(Tl) crystals located inside a superconducting solenoid coil that provides a 1.5 T magnetic field. An iron flux-return located outside of the coil is instrumented to detect K_L mesons and to identify muons (KLM). The detector is described in detail elsewhere [5].

We select events that contain a J/ψ , either a charged or neutral kaon, and a $\pi^+ \pi^-$ pair using criteria described in refs. [1] and [6]. To reduce the level of $e^+e^- \rightarrow q\bar{q}$ ($q = u, d, s$ or c -quark) continuum events in the sample, we also require $R_2 < 0.4$, where R_2 is the normalized Fox-Wolfram moment [7], and $|\cos \theta_B| < 0.8$, where θ_B is the polar angle of the B -meson direction in the cms.

Candidate $B \rightarrow K \pi^+ \pi^- J/\psi$ mesons are identified by the energy difference $\Delta E \equiv E_B^{\text{cms}} - E_{\text{beam}}^{\text{cms}}$ and the beam-energy constrained mass $M_{\text{bc}} \equiv \sqrt{(E_{\text{beam}}^{\text{cms}})^2 - (p_B^{\text{cms}})^2}$, where $E_{\text{beam}}^{\text{cms}}$ is the cms beam energy, and E_B^{cms} and p_B^{cms} are the cms energy and momentum of the $K \pi^+ \pi^- J/\psi$ combination. We select events with $M_{\text{bc}} > 5.20$ GeV and $|\Delta E| < 0.2$ GeV and among these define a signal region $5.2725 \text{ GeV} < M_{\text{bc}} < 5.2875 \text{ GeV}$ and $|\Delta E| < 0.034 \text{ GeV}$; this corresponds to $\pm 3\sigma$ from the central values for each variable.

We select events with a dipion invariant mass requirement of $M_{\pi^+ \pi^-} > (M(\pi^+ \pi^- J/\psi) - (m_{J/\psi} + 200 \text{ MeV}))$, which corresponds to $M_{\pi^+ \pi^-} > 575 \text{ MeV}$ for the $X(3872)$. This reduces misidentified γ conversions and combinatoric backgrounds by 36% with an $X(3872)$ signal loss of 6%.

These selection criteria isolate a very pure sample of 696 ± 26 $B \rightarrow K \psi(2S)$, $\psi(2S) \rightarrow \pi^+ \pi^- J/\psi$ events. These events are used as a calibration reaction to determine the M_{bc} , ΔE and $M(\pi^+ \pi^- J/\psi)$ peak positions and resolution values, and for validating the Monte-Carlo (MC) acceptance calculations.

Figure 1 shows the $M(\pi^+ \pi^- J/\psi)$ mass distribution near 3872 MeV for the selected events. Here the smooth curve is the result of a fit with a Gaussian function to represent the $X(3872)$ signal and a first-order polynomial to represent the background. The width of the Gaussian is fixed at $\sigma = 3.2 \text{ MeV}$, the experimental resolution determined from the $\psi(2S) \rightarrow \pi^+ \pi^- J/\psi$ event sample. The total signal yield is 49.1 ± 8.4 events. For subsequent analysis, we define an $X(3872)$ signal region to be $\pm 5 \text{ MeV}$ around the signal peak. For background estimates, we use $\pm 50 \text{ MeV}$ sidebands above and below the signal peak centered at 3837 MeV and 3907 MeV. There are a total 58 events in the signal region; the background content, determined from the scaled sidebands, is 11.4 ± 1.1 events.

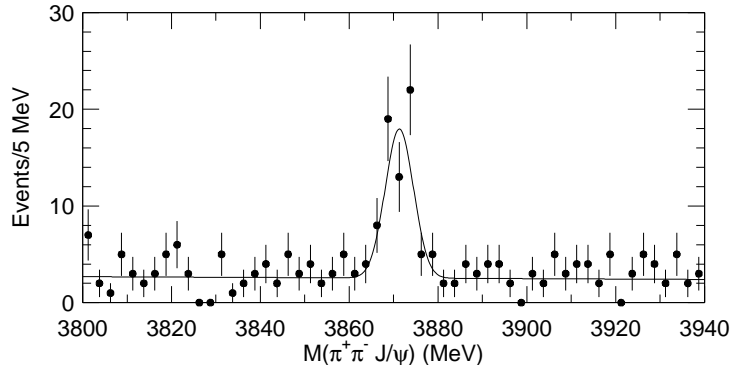


FIG. 1: The $M(\pi^+\pi^- J/\psi)$ mass distribution for the $X(3872)$ region.

Using a MC-determined acceptance, we determine the product branching fraction

$$\mathcal{B}(B \rightarrow KX(3872)) \times \mathcal{B}(X \rightarrow \pi^+\pi^- J/\psi) = 1.31 \pm 0.24(\text{stat}) \pm 0.13(\text{syst}) \times 10^{-5}. \quad (1)$$

where we have assumed equal $B \rightarrow KX$ branching fractions for charged and neutral B mesons, and that the dipion originates from $\rho \rightarrow \pi^+\pi^-$. The systematic error includes the effect of uncertainties in the $M(\pi^+\pi^-)$ shape for $X(3872)$ decay. This result agrees with, and supersedes, the results of ref. [1].

Since both the B and K mesons are scalar particles, $X(3872)$ mesons produced via exclusive $B \rightarrow KX$ decays cannot have a non-zero component of angular momentum along their momentum direction in the B rest frame. This provides useful limits on the number of independent partial-wave amplitudes needed to describe the decay [8, 9, 10].

With less than fifty signal events, any angular distribution will have, on average, only about five signal events per bin, which is not sufficient for a standard angular analysis. However, because the signal-to-noise ratio for the $X \rightarrow \pi^+\pi^- J/\psi$ signal is quite good ($S/N \simeq 4$), a typical distribution has, on average, only about one or two background events per bin. We exploit this good S/N and try to find, for a given J^{PC} hypothesis for the $X(3872)$, angular quantities that have distributions with a zero in some location. In the bins near the zero point, any observed events would have to be accounted for by upward fluctuations of the background [11].

For 0^{-+} , there is only one invariant amplitude corresponding to a ρ and J/ψ in a P -wave. The decay amplitude is proportional to the scalar triple product of the ρ and J/ψ polarizations and their relative momentum. As a result, the polarizations are perpendicular to each other and their relative momentum. We follow a suggestion by Rosner [9] and use a coordinate system where the x -axis is defined to be opposite the J/ψ direction in the ρ rest frame, the $x-y$ plane is defined by the π^+ and J/ψ directions and the z -axis is chosen so that it forms a right-handed coordinate system. We define θ as the angle between the ℓ^+ and the z axis in the J/ψ rest frame and ψ as the angle between the π^+ and the x axis in the dipion rest frame. The expected distribution for 0^{-+} is $d^2N/d(\cos\theta)d(\cos\psi) \propto \sin^2\theta \sin^2\psi$.

The $|\cos\theta|$ and $|\cos\psi|$ distributions for the $X(3872)$ signal region are shown in Figs. 2(a) and (b), respectively. The shaded histograms indicate the side-band determined background. The distributions for both variables show strong signals at the upper edge of each plot, in contrast to expectations for a $\sin^2\theta \sin^2\psi$ dependence. The open histogram shows the 0^{-+}

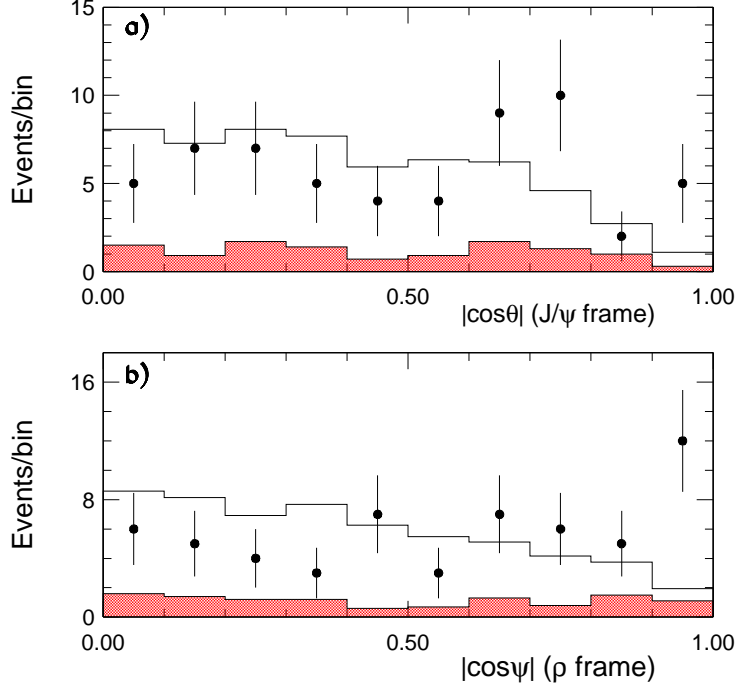


FIG. 2: The (a) $|\cos\theta|$ and (b) $|\cos\psi|$ distributions for events in the $X(3872)$ signal region (points with error bars). The open histogram is the expected distribution for a 0^{-+} assignment including background. The hatched histogram shows the scaled sideband.

MC expectations plus background, normalized to the observed number of events. Here the agreement is marginal for $\cos\theta$: $\chi^2/d.o.f. = 17.7/9$ but poor for $\cos\psi$: $\chi^2/d.o.f. = 34.2/9$. This latter distribution allows us to reject the 0^{-+} assignment with high confidence.

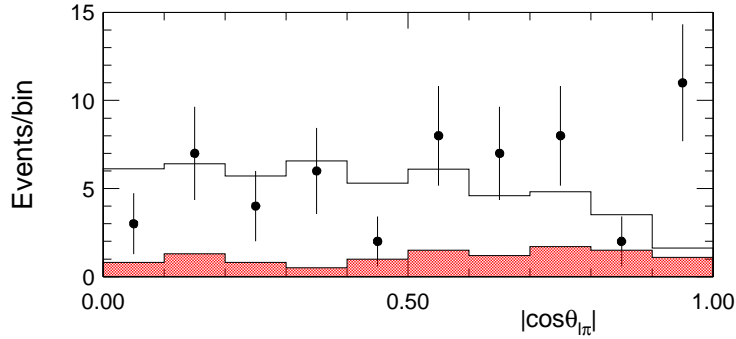


FIG. 3: The $|\cos\theta_{\ell\pi}|$ distribution for events in the $X(3872)$ signal region (points with error bars). The open histogram is the expected distribution for a 0^{++} assignment including background. The hatched histogram shows the scaled sideband.

For 0^{++} , two invariant amplitudes are possible, corresponding to the ρ and J/ψ in relative S - or D -waves. Because of the limited phase-space, the D -wave contribution can be expected to be strongly suppressed relative to the S wave term and is ignored. The amplitude is then proportional to the scalar product of the ρ and J/ψ polarizations. We define $\theta_{\ell\pi}$ as the angle between the ℓ^+ and the π^+ in the $X(3872)$, J/ψ

and ρ rest frames coincide $dN/d(\cos\theta_{\ell\pi}) \propto \sin^2\theta_{\ell\pi}$. The kinematic smearing due to relative motion of the different frames is incorporated in the MC simulations that are used to compare data with expectations [13].

Figure 3 shows the $|\cos\theta_{\ell\pi}|$ distribution, computed in the ρ rest frame, for $X(3872)$ signal region events. The agreement with S -wave 0^{++} MC expectations is poor: $\chi^2/d.o.f. = 31.0/9$, and provides evidence against the 0^{++} assignment.

For 1^{++} the J/ψ and ρ can be in a relative S and/or D -wave. We use a coordinate system [9] where the x -axis is the negative of the kaon flight path, the $x-y$ plane is defined by the kaon and π^+ and the z axis completes a right-handed coordinate system. The angle between the π^+ direction and the x -axis is χ and the angle between the ℓ^+ direction and the z -axis is θ_ℓ . In the limit where the J/ψ and ρ are at rest in the X rest frame (and D -wave contributions can be neglected), the amplitude is proportional to the vector triple product of the X , ρ and J/ψ polarizations, and the choice of axes ensures that the X polarization is along the x direction [9, 10]. The expectation for 1^{++} is $d^2N/d(\cos\theta_\ell)d(\cos\chi) \propto \sin^2\theta_\ell \sin^2\chi$.

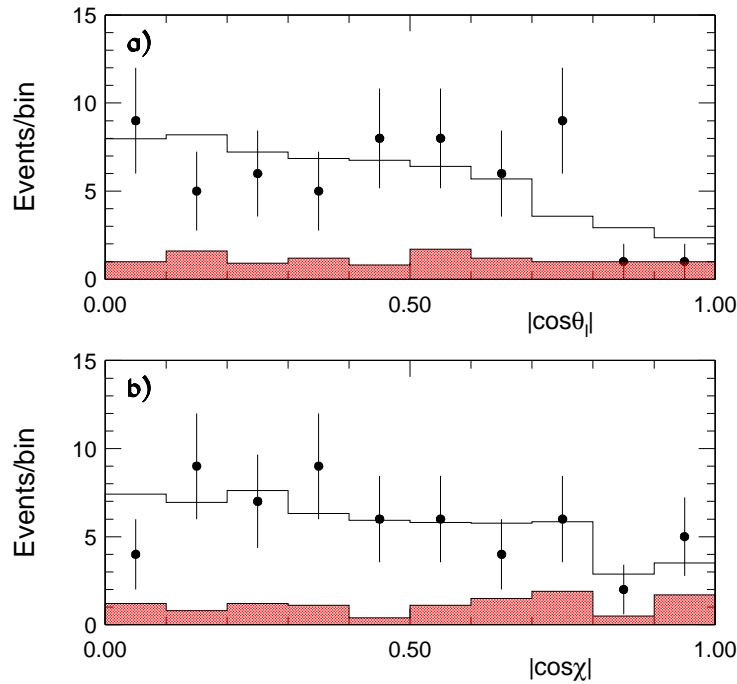


FIG. 4: The **a)** $|\cos\theta_\ell|$ and **b)** $|\cos\chi|$ distribution for events in the $X(3872)$ signal region (points with error bars). The open histogram is the expected distribution for a 1^{++} assignment including background. The hatched histogram shows the scaled sideband.

The $|\cos\theta_\ell|$ distribution for $X(3872)$ signal region events is shown in Fig. 4(a). The distribution tends toward zero at the upper edge of the plot, as expected for a $\sin^2\theta_\ell$ dependence. The open histogram shows the results of a comparison to normalized MC expectations for 1^{++} decaying to a ρ and J/ψ in an S -wave. The agreement is good: $\chi^2/d.o.f. = 11.4/9$. The $|\cos\chi|$ distribution is shown in Figs. 4(b) together with the MC expectation for 1^{++} . The agreement here is also good: $\chi^2/d.o.f. = 5.0/9$.

For even-parity $C = +1$ states the $\pi^+\pi^-J/\psi$ final state would be a ρ and J/ψ primarily in a relative S -wave, with some possible D -wave component. For odd-parity states the ρ and J/ψ would be in a relative P -wave with some possible F -wave. The $M(\pi^+\pi^-)$ mass

distribution near the upper kinematic boundary is suppressed by a $(q_{J/\psi}^*)^{2\ell+1}$ centrifugal barrier, where $q_{J/\psi}^*$ is the J/ψ momentum in the $X(3872)$ rest frame, and ℓ is the orbital angular momentum. For the S -wave (*i.e.* $J^P = J^+$) cases, the upper-boundary is modulated by the available phase-space, which is proportional to $q_{J/\psi}^*$; for a P -wave the modulation is $(q_{J/\psi}^*)^3$. Thus, the shape of the high-mass part of the $\pi^+\pi^-$ invariant mass distribution provides some J^{PC} information.

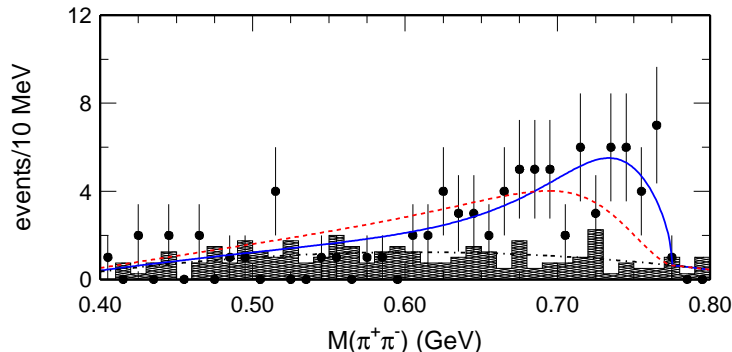


FIG. 5: $M(\pi^+\pi^-)$ distribution for events in the $X(3872)$ signal region; the histogram indicates the side-band determined background. The solid (dashed) curve shows the fit that uses a ρ Breit-Wigner line shape with the J/ψ and ρ in a relative S -wave (P -wave). The dot-dashed curve is a smooth parameterization of the background that is used in the fit.

Figure 5 shows the distribution for events in the $X(3872) \rightarrow \pi^+\pi^-J/\psi$ signal region with the $M(\pi^+\pi^-)$ requirement relaxed; the histogram indicates the side-band determined background, which is parameterized by the fourth-order polynomial shown in the figure as a dot-dashed curve. The solid curve in Fig. 5 shows the result of a fit to the $M(\pi^+\pi^-)$ distribution that uses the background function plus an acceptance-weighted ρ BW line-shape with an S -wave cut-off factor at the upper kinematic boundary [14]; the dashed curve shows the fit with a P -wave cut-off factor. The S -wave case fits the data well: $\chi^2/d.o.f. = 43.1/39$ (CL=28%). The P -wave fit is much poorer, $\chi^2/d.o.f. = 71.0/39$ (CL=0.1%), indicating that J^{++} is strongly favored over J^{-+} .

In summary, we find that with reasonable assumptions and a sample of 47 $X \rightarrow \pi^+\pi^-J/\psi$ signal events, we can rule out the $J^{PC} = 0^{-+}$ and 0^{++} assignments for the $X(3872)$ based on angular correlations among the final state particles. In addition, the $M(\pi^+\pi^-)$ distribution is inconsistent with all J^{-+} assignments.

The results reported here, taken together with the observation of the $X(3872) \rightarrow \gamma J/\psi$ decay mode [3], rule out all J^{PC} assignments with $J \leq 2$ other than 1^{++} and 2^{++} . The decay angular distributions and $\pi^+\pi^-$ invariant mass distribution agree well with expectations for the 1^{++} assignment. The 2^{++} assignment is not seriously challenged by any of the tests reported here, but is made rather unlikely by Belle's recently reported evidence for the decay $X(3872) \rightarrow D^0\bar{D}^0\pi^0$ [15]. The formation of 2^{++} from three pseudoscalars requires at least one combination to be in a D -wave. Thus, the near-threshold production of $D^0\bar{D}^0\pi^0$ would be suppressed by an $\ell = 2$ centrifugal barrier.

The 1^{++} charmonium χ'_{c1} state is an unlikely assignment for the $X(3872)$. Potential model predictions for the χ'_{c1} mass range from 3953 MeV \sim 3990 MeV [16], well above the $X(3872)$ mass. The potential model masses are expected to be modified by coupling to

open-charm states. A coupled-channel calculation of open-charm-induced splittings for the χ'_{c1} yields an upward mass shift of +28 MeV [17].

The decay $\chi'_{c1} \rightarrow \pi^+\pi^-J/\psi$ would proceed via $\rho J/\psi$ and violate isospin. The only well established isospin-violating hadronic transition in the charmonium system is $\psi(2S) \rightarrow \pi^0 J/\psi$, which has a measured partial width of $\Gamma(\psi(2S) \rightarrow \pi^0 J/\psi) = 0.27 \pm 0.06$ keV [12]. This is small compared to the expected total width of an $M = 3872$ MeV χ'_{c1} of more than 1 MeV [16, 17]. A decay mode with a partial width this small would thus have a branching fraction that is less than 0.1%. This contradicts the recent BaBar 90% confidence lower limit of $\mathcal{B}(X(3872) \rightarrow \pi^+\pi^-J/\psi) > 4.3\%$ [18]. Godfrey and Barnes calculate a partial width for an $M = 3872$ MeV χ'_{c1} to be 11 KeV [16], more than an order-of-magnitude larger than that for the isospin violating $\psi(2S) \rightarrow \pi^0 J/\psi$ transition. Thus, one expects the $\gamma J/\psi$ decay to be stronger than $\rho J/\psi$. This is contradicted by our measurement: $\Gamma(X(3872) \rightarrow \gamma J/\psi)/\Gamma(X(3872) \rightarrow \pi^+\pi^-J/\psi) = 0.14 \pm 0.05$ [3].

The 1^{++} assignment is favored by models that treat the $X(3872)$ as a molecule-like $D^0\bar{D}^{*0}$ bound state [19, 20]. These models predict strong isospin violations and a $\gamma J/\psi$ branching fraction that is much less than that for $\pi^+\pi^-J/\psi$ [21], in agreement with observations.

We thank the KEKB group for the excellent operation of the accelerator, the KEK Cryogenics group for the efficient operation of the solenoid, and the KEK computer group and the National Institute of Informatics for valuable computing and Super-SINET network support. We acknowledge support from the Ministry of Education, Culture, Sports, Science, and Technology of Japan and the Japan Society for the Promotion of Science; the Australian Research Council and the Australian Department of Education, Science and Training; the National Science Foundation of China under contract No. 10175071; the Department of Science and Technology of India; the BK21 program of the Ministry of Education of Korea and the CHEP SRC program of the Korea Science and Engineering Foundation; the Polish State Committee for Scientific Research under contract No. 2P03B 01324; the Ministry of Science and Technology of the Russian Federation; the Ministry of Education, Science and Sport of the Republic of Slovenia; the National Science Council and the Ministry of Education of Taiwan; and the U.S. Department of Energy.

-
- [1] S.K. Choi *et al.* (Belle Collaboration), Phys. Rev. Lett. **91**, 262001 (2003).
 - [2] The inclusion of charge-conjugate modes is always implied.
 - [3] S.K. Choi *et al.* (Belle Collaboration), BELLE-CONF-0540, hep-ex/0505037.
 - [4] S. Kurokawa and E. Kikutani, Nucl. Instr. and Meth. A499, 1 (2003), and other papers included in this volume.
 - [5] A. Abashian *et al.* (Belle Collaboration), Nucl. Instr. and Meth. A **479**, 117 (2002) and Y. Ushiroda (Belle SVD2 Group), Nucl. Instr. and Meth.A **511**, 6 (2003).
 - [6] S.-K. Choi *et al.* (Belle Collaboration), Phys. Rev. Lett. **94**, 182002 (2005).
 - [7] G.C. Fox and S. Wolfram, Phys. Rev. Lett. **41**, 1581 (1978).
 - [8] S. Pakvasa and M. Suzuki, Phys. Lett. B **579**, 67 (2004).
 - [9] J.L. Rosner, Phys. Rev. D **70**, 094023 (2004).
 - [10] D.V. Bugg, Phys. Rev. D **71**, 016006 (2005).
 - [11] We follow the PDG-recommended procedure for hypothesis testing with small statistics samples and use $\chi^2 = -2\ln\lambda$, where λ is defined in Eq. 32.12 of the PDG review [12]. The distribution of this statistic is found to approach the asymptotic limit faster than other χ^2

- statistics.
- [12] S. Eidelman *et al.* (Particle Data Group), Phys. Lett. B **592**, 1 (2004).
 - [13] The $\cos \theta_{\ell\pi}$ distributions calculated in the X , J/ψ and ρ rest frames have similar shapes; the difference distributions have an rms spread of $\simeq 0.2$.
 - [14] T. Kim and P. Ko, Phys. Rev. D **71**, 034025 (2005).
 - [15] G. Gokhroo *et al.* (Belle Collaboration), BELLE-CONF-0568 (2005).
 - [16] T. Barnes and S. Godfrey, Phys. Rev. D **69**, 054008 (2004).
 - [17] E.J. Eichten, K. Lane and C. Quigg, Phys. Rev. D **69**, 094019 (2004).
 - [18] J. Coleman (BaBar Collaboration), talk at the 2005 Rencontre de Moriond on QCD and Hadronic Interactions, March 2005.
 - [19] N.A. Törnqvist, Phys. Lett. B **590**, 209 (2004).
 - [20] E.S. Swanson, Phys. Lett. B **588**, 189 (2004).
 - [21] E.S. Swanson, Phys. Lett. B **598**, 197 (2004).